Title

cGMP-dependent protein kinase-2 regulates bone mass and prevents diabetic bone loss

Journal

Journal of Endocrinology, 238(3)

ISSN

0022-0795

Authors

Ramdani, Ghania
Schall, Nadine
Kalyanaraman, Hema
et al.

Publication Date

2018-09-01

DOI

10.1530/joe-18-0286

Peer reviewed

HHS Public Access

Author manuscript

J Endocrinol. Author manuscript; available in PMC 2019 September 01.

Published in final edited form as:

J Endocrinol. 2018 September ; 238(3): 203–219. doi:10.1530/JOE-18-0286.

cGMP-dependent Protein Kinase-2 Regulates Bone Mass and Prevents Diabetic Bone Loss

Ghania Ramdani[1], **Nadine Schall**[1,2], **Hema Kalyanaraman**[1], **Nisreen Wahwah**[1], **Sahar Moheize**[1], **Jenna J. Lee**[3], **Robert L. Sah**[3], **Alexander Pfeifer**[2], **Darren E. Casteel**[1], and **Renate B. Pilz**[1,4]

[1]Department of Medicine, University of California, San Diego, La Jolla, CA 92093-0652, USA

[2]Institute for Pharmacology and Toxicology, University of Bonn, 53105 Bonn, Germany

[3]Department of Bioengineering, University of California, San Diego, La Jolla, CA 92093-0652, USA

Abstract

NO/cGMP signaling is important for bone remodeling in response to mechanical and hormonal stimuli, but the downstream mediator(s) regulating skeletal homeostasis are incompletely defined. We generated transgenic mice expressing a partly-activated, mutant cGMP-dependent protein kinase type 2 ($PKG2^{R242Q}$) under control of the osteoblast-specific Col1a1 promoter to characterize the role of PKG2 in post-natal bone formation. Primary osteoblasts from these mice showed a 2- to 3-fold increase in basal and total PKG2 activity; they proliferated faster and were resistant to apoptosis compared to cells from wild type mice. Male Col1a1-$Prkg2^{R242Q}$ transgenic mice had increased osteoblast numbers, bone formation rates, and Wnt/β-catenin-related gene expression in bone, and a higher trabecular bone mass compared to their wild type litter mates. Streptozotocin-induced type 1 diabetes suppressed bone formation and caused rapid bone loss in wild type mice, but male transgenic mice were protected from these effects. Surprisingly, we found no significant difference in bone micro-architecture or Wnt/β-catenin-related gene expression between female wild type and transgenic mice; female mice of both genotypes showed higher systemic and osteoblastic NO/cGMP generation compared to their male counterparts, and a higher level of endogenous PKG2 activity may be responsible for masking effects of the $PKG2^{R242Q}$ transgene in females. Our data support sexual dimorphism in Wnt/β-catenin signaling and PKG2 regulation of this crucial pathway in bone homeostasis. This work establishes PKG2 as a key regulator of osteoblast proliferation and post-natal bone formation.

[4]CORRESPONDING AUTHOR: Renate B. Pilz, rpilz@ucsd.edu, University of California, San Diego, 9500 Gilman Dr., La Jolla, CA 92093-0652. Phone: 858-534-8805, Fax: 858-534-1421.

Conflict of Interest: The authors declare that they have no conflicts of interest with the contents of this article. The content of the manuscript is solely the responsibility of the authors and does not necessarily represent the official views of the National Institutes of Health.

Authors' Contributions: Study design: RBP and GR. Study conduct: GR, NS, HK, NW, JC, DEC, SM, and EC. Data collection: GR, NS, HK, and EC. Data analysis: GR, HK, RLS, and RBP. Data interpretation: RBP, GR, HK, and RLS. Drafting manuscript: GR and RBP. RBP and GR take responsibility for the integrity of the data analysis.

Keywords

cGMP-dependent protein kinase; osteoblasts; bone formation; diabetic osteoporosis; Wnt pathway; sexual dimorphism

INTRODUCTION

Cyclic GMP is produced by two types of guanylyl cyclases (GCs): receptor GCs activated by peptide ligands such as C-type natriuretic peptide (CNP) and soluble GCs activated by nitric oxide (NO) (Hofmann *et al.* 2009; Kuhn 2016; Hannema *et al.* 2013). cGMP regulates ion channels, phosphodiesterases, and two types of cGMP-dependent protein kinases (PKG1 and 2), encoded by two homologous genes (*Prkg*1 and 2) (Hofmann *et al.* 2009). PKG1 is widely expressed with high levels found in the vasculature, whereas PKG2 expression is limited to specific cell types in bone, intestine, brain, and kidney (Vaandrager *et al.* 2005). PKG1 and 2 are both found in osteoblasts and chondroblasts (Pfeifer *et al.* 1996; Rangaswami *et al.* 2009).

The CNP/GC-B/PKG2 pathway regulates endochondral ossification, responsible for fetal skeletal development and post-natal longitudinal bone growth. Loss-of function mutations or genetic ablation of CNP, GC-B, or PKG2 cause dwarfism in humans and rodents, while increased CNP expression or a gain-of-function mutation in GC-B cause long bone over-growth (Hannema *et al.* 2013; Chusho *et al.* 2001; Bartels *et al.* 2004; Bonnet *et al.* 2010; Bocciardi *et al.* 2007; Miura *et al.* 2012; Pfeifer *et al.* 1996).

The NO/soluble GC pathway regulates adult skeletal homeostasis: NO is required for the anabolic response of bone to mechanical stimulation and regulates bone remodeling downstream of estrogens and thyroid hormone (Kalyanaraman *et al.* 2018a; Rangaswami *et al.* 2010; Watanuki *et al.* 2002; Kalyanaraman *et al.* 2017; Kalyanaraman *et al.* 2014). Some strains of NOS3-deficient mice have reduced bone mass due to defects in osteoblast number and maturation, whereas other strains only show exaggerated bone loss after ovariectomy (OVX) and a blunted response to estrogens (Armour *et al.* 2001; Aguirre *et al.* 2001; Grassi *et al.* 2006). Treatment with NO-generating agents and NO-independent soluble GC activators prevents bone loss from estrogen deficiency and type 1 diabetes, respectively (Wimalawansa *et al.* 1996; Kalyanaraman *et al.* 2017; Wimalawansa 2000; Nabhan & Rabie 2008; Jamal *et al.* 2004; Kalyanaraman *et al.* 2018b).

We have shown *in vitro* that PKG1 and 2 are both targets of NO and cGMP in osteoblasts and osteocytes, with largely distinct functions: PKG2 mediates pro-proliferative effects of insulin and mechanical stimulation, while PKG1 and 2 both mediate pro-survival effects of estrogens via distinct mechanisms (Rangaswami *et al.* 2009; Marathe *et al.* 2012; Rangaswami *et al.* 2010; Kalyanaraman *et al.* 2018b). PKG2 regulates nuclear translocation of β-catenin, a transcriptional co-activator downstream of the Wnt co-receptor low-density lipoprotein receptor-related protein-5 (LRP5), which plays a central role in skeletal homeostasis (Rangaswami *et al.* 2012; Kalyanaraman *et al.* 2017; Baron & Kneissel 2013). NO and cGMP also regulate osteoclast motility and acid secretion via PKG1; however, some

NO effects in bone are cGMP-independent (Kalyanaraman *et al.* 2018a; Wimalawansa 2007; van't Hof & Ralston 2001).

To examine the role of PKG2 in post-natal bone acquisition, independently of its function in endochondral bone formation, we established transgenic mice expressing a novel PKG2 mutant with increased basal kinase activity under control of the 2.3 kb Col1a1 promoter; the promoter is specific for cells of osteoblast lineage and has no detectable activity in osteoclasts (Kalajzic *et al.* 2002; Dacquin *et al.* 2002). The transgenic mice exhibited gender-specific increases in trabecular bone volume and Wnt//β-catenin-related gene expression in bone. We detected higher NO and cGMP concentrations in serum and osteoblasts from female compared to male mice, which at least partly explain the sexually dimorphic skeletal phenotype of Col1a1-prkg2^{RQ} transgenic mice. To avoid the influence of estrogen on NO/cGMP/PKG signaling, we then focused on male mice and found that male transgenic mice are protected from diabetes-induced bone loss.

MATERIALS AND METHODS

Materials

Antibodies against Akt, Akt(pSer^{473}), Erk1(pTyr^{204}), GSK-3β(pSer^{9}), VASP(pSer^{239}), NOS-3(pSer^{1177}), caveolin-1, and cleaved caspase-3 were from Cell Signaling Technology. Antibodies against PKG2 and β-catenin, and FITC-labeled secondary antibodies were from Invitrogen. A second monoclonal mouse antibody against PKG2, and a β-actin antibody were from Santa Cruz Biotechnology. 8-(4-chlorophenylthio)-cGMP (8-pCPT-cGMP) was from BioLog. The IP3-receptor peptide GRRESLTSFG was synthesized by Eton Bioscience.

Generation of Col1a1-Prkg2^{RQ} transgenic mice

A 2.3 kb segment of the mouse type Ia collagen (Col1a1) promoter, including the transcription start site and a short 5′-untranslated sequence (Yuen *et al.* 1989), was amplified by PCR using the following primers: 5′-attCCTAGGCTGCCTCTGCTTCTGTTCCA-3′ and 5′-aatgcggccgcATGCCACGTGTAAAGG-3′ (including a NotI fusion site). A rat *Prkg2* cDNA encoding PKG2 with a R242Q mutation (hereafter referred to as *Prkg2*^{RQ} or PKG2^{RQ}) was generated by site-directed mutagenesis (Zhao *et al.* 2005). We did not add an N-terminal epitope tag to avoid problems with enzyme mis-localization (Vaandrager *et al.* 1996), and we found that C-terminal tags reduce kinase activity. The Col1a1-*Prkg2*^{RQ} transgenic construct was generated by fusing the 2.3 kb Col1a1 promoter with the entire coding sequence of the rat *Prkg2*^{RQ} cDNA, followed by a SV40 polyadenylation sequence. The construct was sequenced, and purified DNA micro-injected into pronuclei of fertilized eggs from C57BL/6 mice. Presence of the transgene in offsprings was detected by PCR analysis of tail DNA using the primers 5′CGAGCCGAAAGAGTCTACA3′ (F1) and 5′GTCTTGAAGTCCTCGCGCTCATGG3′ (R1). Mice hemizygous for the Col1a1-prkg2^{RQ} transgene were bred with wild type C57BL/6 mice from Harlan (Cumberland,IN).

Animal experiments

All mouse experiments were approved by the Institutional Animal Care and Use Committee of the University of California, San Diego. Mice were housed in a temperature-controlled

environment with a 12 hour light/dark cycle and *ad libitum* access to water and food (Teklad Rodent Diet #8604). To induce insulin deficiency (type 1 diabetes), 6 week-old wild-type (n=18) and transgenic (n=16) male litter mates were randomly assigned to receive two intraperitoneal injections of streptozotocin (STZ, 100 mg/kg/d) or vehicle on two consecutive days (after 4 h of fasting). Twelve days later, glucose was measured in tail vein blood and mice with blood glucose concentrations ≥ 15 mM were considered diabetic; three STZ-injected mice with glucoses < 15 mM were excluded. Double calcein labeling was performed by intraperitoneal injection of calcein (25mg/kg) at 7 and 2 d before euthanasia by CO_2 intoxication and exsanguination.

Primary osteoblast (POB) cultures and proliferation assays

POBs were isolated from femurs and tibiae of 8 week-old mice and were cultured as described (Kalyanaraman *et al.* 2014). To induce differentiation, cells were plated at high density, and after confluency were switched to medium with 0.3 mM sodium ascorbate and 10 mM β-glycerophosphate. Each POB preparation was characterized by alkaline phosphatase (ALP) staining and mineralization capacity as described (Kalyanaraman *et al.* 2014); cells were used at passages 1–3 and counted using a T20 automated cell counter (BioRad). Metabolically-active osteoblasts were quantified using a CellTiter 96® AQ_{ueous} Cell Proliferation Assay Kit (Promega): after 16 h in medium with 0.1% FBS, cells were stimulated with 10% FBS for 24 h, and MTS reduction to formazan was measured spectrophotometrically over 4 h.

Bone marrow stromal cell (BMSC) cultures

Bone marrow mononuclear cells were plated at 4×10^5 cells/cm^2 in RPMI 1640 with 10% FBS and 10% horse serum (Joshua *et al.* 2014). After seven days, adherent cells were switched to α-MEM supplemented with 10% FBS/10% horse serum, 0.3 mM sodium ascorbate, and 10 mM β-glycerolphosphate to induce differentiation. ALP and Alizarin Red staining was performed 14 d and 21 d later, respectively; colonies were counted and stained area was quantified by ImageJ (Joshua *et al.* 2014; Kalyanaraman *et al.* 2014).

PKG2 purification and activity assays

Wild type PKG2 and mutant $PKG2^{RQ}$ were expressed with N-terminal Flag epitope-tags in transiently-transfected 293T cells, purified on anti-Flag beads, and eluted with Flag peptide (Kalyanaraman *et al.* 2014). Kinase activity was measured using the synthetic peptide GRRESLTSFG and [γ-^{32}P]ATP in the absence and presence of cGMP (Zhao *et al.* 2005). POB plasma membranes were isolated by density-gradient centrifugation (Kalyanaraman *et al.* 2014).

Quantitative RT-PCR

After removing growth plates and bone marrow, bone shafts were snap-frozen and pulverized. RNA was purified with RNeasy Mini-Kit columns (Qiagen). Quantitative RT-PCR was performed with 300 ng of RNA as described (Kalyanaraman *et al.* 2017). All primers (Supplemental Table 1) were tested with serial cDNA dilutions. Genes of interest were normalized to three different reference genes: *18S* rRNA, *Hprt*, and *B2m*. The mean

ΔCT obtained for control wild type mice was used to calculate the fold change in mRNA expression in the transgenic group using the ΔΔCT method; for each mouse the fold change in mRNA expression obtained using the different reference genes was averaged.

Western blotting, immunofluorescence and immunohistochemical staining

Western blots were generated using horseradish peroxidase-conjugated secondary antibodies detected by enhanced chemiluminescence (Rangaswami *et al.* 2009). POBs plated on glass coverslips were fixed in 4% paraformaldehyde, permeabilized with 1% Triton-X-100, and incubated with PKG2 antibody (1:100) or cleaved caspase-3–specific antibody (1:100 dilution), followed by a secondary FITC-conjugated antibody. Nuclei were counterstained with Hoechst 33342, and images were analyzed with a Keyence BZ-X700 fluorescence microscope.

Tibiae were fixed overnight in 10% formalin, decalcified in 0.5M EDTA (pH 7.5) for 5 d, and embedded in paraffin. Eight μm sections were de-paraffinized in xylene and rehydrated in graded ethanol and water. For antigen retrieval, slides were placed in 10 mM sodium citrate buffer (pH 6.0) at 80–85°C, and allowed to cool to room temperature for 30 min. Endogenous peroxidase activity was quenched in 3% H_2O_2 for 10 min. After blocking with 5% normal goat serum, slides were incubated overnight at 4°C with anti-PKG2 antibody (1:100), followed by a horseradish peroxidase-conjugated secondary antibody. After development with 3-diaminobenzidine (Vector Laboratories), slides were counterstained with hematoxylin.

Quantitation of NO_x and cGMP

NO production was measured as the sum of nitrite and nitrate accumulation in the medium or serum, using a two-step colorimetric assay as described (Kalyanaraman *et al.* 2018b). cGMP concentrations were measured using an ELISA kit according to the manufacturer's protocol (Biomedical Technologies).

Micro-CT

Ethanol-fixed tibiae were analyzed according to established guidelines (Bouxsein *et al.* 2010), using a Skyscan 1076 (Skyscan, Belgium) scanner at 9 μm voxel size, and applying an electrical potential of 50 kVp and current of 200 mA, with a 0.5-mm aluminum filter as described (Kalyanaraman *et al.* 2017). Mineral density was determined by calibration of images against 2-mm diameter hydroxyapatite rods (0.25 and 0.75 g/cm^3). Cortical bone was analyzed by automatic contouring 3.6 to 4.5 mm distal to the proximal growth plate, using a global threshold to identify cortical bone, and eroding one pixel to eliminate partial volume effects. Trabecular bone was analyzed by automatic contouring of the proximal tibial metaphysis (0.36 to 2.1 mm distal to the growth plate), using an adaptive threshold to select the trabecular bone (Kalyanaraman *et al.* 2017).

Histomorphometry

Femurs were fixed in 70% ethanol, dehydrated and embedded in methyl methacrylate, and sectioned at the University of Alabama Center for Metabolic Bone Disease. Masson's Trichrome-stained sections were used for static parameters, and unstained sections were

used to assess fluorochrome labeling. Slides were scanned with a Hamamatsu Nanozoomer 2.0 HT Slide Scanning System (Hamamatsu Corporation), and image analysis was performed using the Nanozoomer Digital Pathology NDP.view2 software. Trabecular bone was analyzed between 0.25 and 1.25 mm, and cortical bone between 0.25 and 5 mm proximal to the growth plate by an observer blinded to the genotype of the mice (Joshua *et al.* 2014).

Statistical Analyses

GraphPad Prism5 was used for two-tailed Student t-test (to compare two groups) or one-way ANOVA with Bonferroni post-test (to compare more than two groups); $p<0.05$ was considered significant. When analyzing bone micro-architecture in diabetic mice, we tested the following primary and secondary hypotheses by two-sided t-test: (i) Transgenic animals are protected from diabetic bone loss; (ii) wild type diabetic animals have lower bone mass compared to non-diabetic wild type animals; and (iii) transgenic animals have higher bone mass compared to wild type animals.

RESULTS

Generation of transgenic mice with expression of a mutant PKG2^{R242Q} from the Col1a1 promoter [Col1a1-*Prkg2*^{RQ}]

To delineate *in vivo* functions of PKG2 in osteoblasts, we introduced a mutation in the first cGMP binding domain of PKG2, homologous to a gain-of-function mutation in PKG1 associated with human thoracic aortic aneurysms and dissections (Guo *et al.* 2013). In contrast to the R177Q mutation in PKG1—which causes nearly complete activation and renders the enzyme largely cGMP-unresponsive (Guo *et al.* 2013)—the PKG2 R242Q mutation increased basal activity of the purified enzyme only about four-fold, to <10% of maximal cGMP-stimulated activity (Fig. 1A,B and Suppl. Fig. 1A). Both mutations are located in the first cGMP binding pocket and likely disrupt interaction between inhibitory and catalytic domains, but the relative cGMP affinities of the first and second cGMP binding pockets are reversed between PKG1 and 2 (Vaandrager *et al.* 2005)—the first cGMP binding site in PKG2 is a low affinity, rapidly-dissociating site, which may explain the less dramatic effect of the mutation in PKG2.

The mutant PKG2^{RQ} was cGMP responsive with a similar cGMP affinity as the wild type enzyme (K_a = 0.4 and 0.45 μM, respectively). Similarly, the mutant enzyme's affinity for a synthetic peptide substrate was similar to that of the wild type enzyme (Suppl. Fig. 1B). We chose to express mutant PKG2^{RQ} under control of the murine 2.3 kb Col1a1 promoter, because the latter is active in cells of the osteoblastic lineage, starting from committed mesenchymal stem cells through mature osteocytes (Kalajzic *et al.* 2002; Dacquin *et al.* 2002). One of several transgenic founder lines was further characterized (Line Fe-9, Suppl. Fig. 1C).

Osteoblast-specific PKG2^{RQ} expression in Col1a1-*Prkg2*^{RQ} transgenic mice

PCR analysis of reverse-transcribed RNA extracted from multiple organs showed amplification of a specific, 210 bp band corresponding to the transgene-derived *Prkg2*^{RQ}

mRNA in bone, but not in other organs (Fig. 1D); this band was not detected in the absence of reverse transcriptase, thus excluding genomic DNA contamination. Using a primer pair recognizing both mouse (endogenous) and rat (transgenic) *Prkg2* transcripts, we found that the transgenic transcript was expressed ~35-fold higher in bone from transgenic mice compared to the endogenous *Prkg2* transcript in wild type mice. In contrast, wild type and transgenic mice showed similar *Prkg2* mRNA expression in brain and kidney, two organs with high endogenous PKG2 mRNA expression (Vaandrager *et al.* 2005) (Fig. 1E).

Since PKG2 associates with plasma membranes, whereas PKG1 is predominantly cytoplasmic (Vaandrager *et al.* 1996; Hofmann *et al.* 2009; Rangaswami *et al.* 2009), we measured PKG activity in purified plasma membranes of primary osteoblasts (POBs) isolated from wild type and transgenic mice. cGMP-stimulated PKG activity was only about three-fold higher in plasma membranes from transgenic compared to wild type mice, correlating with an increased amount of PKG2 protein (Fig. 1F and Suppl. Fig. 1D). We could not reliably determine basal PKG2 activity in the absence of cGMP using this kinase assay, because available PKG inhibitors are not effective against the mutant PKG2, and the synthetic peptide can be phosphorylated by other membrane-associated kinases. Using a second PKG2-specific antibody, approximately three-fold more PKG2 protein could be detected in whole cell lysates of transgenic compared to wild type POBs (Fig. 1G,H). Correspondingly, phosphorylation of vasodilator-stimulated phosphoprotein (VASP) on Ser^{239}, a site specifically targeted by PKG1 and 2, was increased in transgenic compared to wild type POBs, both in the absence and presence of cGMP (representing basal and maximal PKG activity, respectively) (Fig. 1G,H). Immunofluorescence staining of PKG2 in POBs from transgenic mice was considerably brighter than that of wild type POBs (Fig. 1I). Immunohistochemical staining of bone sections showed a stronger signal in bone-lining osteoblasts in the transgenic compared to wild type mice (Fig. 1J; transgenic mice had more bone-lining osteoblasts than wild type mice; described below and shown in Fig. 5D). However, staining of endogenous PKG2 in megakaryocytes was similar between transgenic and wild type animals (Fig. 1J). Thus, Col1a1-*Prkg2*^{RQ} mice express the mutant PKG2 in osteoblasts, leading to a moderate increase in both basal and cGMP-stimulated PKG2 activity.

Increased proliferation, Erk and Akt/GSK-3/β-catenin signaling in POBs from Col1a1-*Prkg2*^{RQ} transgenic mice

NO/cGMP activation of PKG is required for osteoblasts to proliferate in response to insulin or mechanical stimulation (Rangaswami *et al.* 2010; Kalyanaraman *et al.* 2018b). To examine whether expression of PKG2^{RQ} in osteoblasts affects proliferation, we compared multiple POB cultures that were independently established from 8 week-old Col1a1-*Prkg2*^{RQ} transgenic mice and their wild type litter mates. The population doubling time of male transgenic POBs was 1.5 ± 0.1 d compared to 3.2 ± 0.9 d for wild type cells (Fig. 2A). We also quantified metabolically-active cells after 24 h of serum stimulation by measuring tetrazolium (MTS) reduction to formazan. Male transgenic POBs reduced 45% more MTS than wild type POBs (Fig. 2B). For comparison, POBs isolated from female transgenic mice reduced 18% more MTS than POBs from female wild type litter mates (Suppl. Fig. 2A).

PKG activation by NO/cGMP in osteoblasts leads to activation of ERK and Akt via Src: PKG2 directly phosphorylates and stimulates the phosphatase SHP-1, which de-phosphorylates Src on an inhibitory site (Rangaswami *et al.* 2010; Rangaswami *et al.* 2012). In contrast, PKG2 inactivates GSK-3β both directly, via phosphorylation of a negative-regulatory site, and indirectly, via Akt activation (Rangaswami *et al.* 2012; Kalyanaraman *et al.* 2017). To assess effects of transgenic PKG2^{RQ} expression on ERK, Akt, and GSK-3β phosphorylation, we compared three independent POB lines of male and female wild type and transgenic mice (12 lines total). POBs from male transgenic mice showed significantly higher basal ERK and Akt phosphorylation, and higher cGMP-stimulated ERK, Akt, and GSK-3β phosphorylation compared to POBs from male wild type littermates (Fig. 2C–F). In POBs from female transgenic mice, cGMP-induced ERK phosphorylation was also increased, but Akt and GSK-3β showed only a trend towards increased phosphorylation compared to female wild type mice, and basal phosphorylation was the same between both genotypes in the females (Suppl. Fig. 2B–E). As described above, PKG2 expression was similar in male and female transgenic POBs (Fig. 1G and Suppl. Fig. 2B).

PKG2 directly and indirectly (via Akt activation) inhibits GSK-3β, thereby regulating β-catenin stability and nuclear translocation (Zhao *et al.* 2005; Kalyanaraman *et al.* 2017; Rangaswami *et al.* 2012). In POBs from male Col1a1-*Prkg2*^{RQ} transgenic mice, more nuclei stained positive for β-catenin, under both basal and cGMP-stimulated conditions, compared to cells from wild type mice (Fig. 2G). In contrast, POBs isolated from female transgenic and wild type mice showed similar nuclear β-catenin staining under both basal and cGMP-stimulated conditions (Suppl. Fig. 2F). However, the number of β-catenin-positive nuclei was almost twice as high in unstimulated female compared to male wild type POBs (Fig. 2G and Suppl. Fig. 2F). Interestingly, when basal NO synthesis in female wild type POBs was inhibited with N(ω)-nitro-l-arginine methyl ester (L-NAME), the percentage of β-catenin-positive nuclei was reduced to levels found in male cells (Suppl. Fig. 2G). These data confirm that nuclear localization of β-catenin is under control of NO (Kalyanaraman *et al.* 2017), and suggest a higher level of basal β-catenin signaling in female compared to male osteoblasts, which appears to obscure the PKG*2*^{RQ} effect on β-catenin in female cells (Suppl. Fig. 2F).

Apoptosis resistance and enhanced expression of osteoblast differentiation-associated genes in POBs and BMSCs from male Col1a1-*Prkg2*^{RQ} transgenic mice

POBs from male Col1a1-*Prkg2*^{RQ} transgenic mice showed enhanced survival after prolonged serum starvation: compared to wild type cells, fewer transgenic POBs staining positive for cleaved caspase-3 (Fig. 2H). To examine osteoblast differentiation, POBs from wild type and transgenic mice were plated at high density, and switched to differentiation medium after reaching confluency. Differentiated POBs from male transgenic mice expressed higher amounts of mRNA encoding β-catenin (C*tnnb1*), collagen-1α (C*ol1a1*), and osteocalcin (*Bglap*) compared to wild type POBs, while expression of *Runx2* and β-actin (*Actb*) was unchanged (Fig. 2I). However, POBs of both genotypes showed similar ALP activity and mineralization after 14 and 21 d, respectively (Suppl. Fig. 3A,B).

To examine the effect of $PKG2^{RQ}$ expression on osteoblast progenitors, we cultured BMSCs from male wild type and Col1a1-*Prkg2*^{RQ} transgenic mice in osteoblastic differentiation medium. We found the same number and size of colonies staining positive for ALP activity, and the same degree of mineralization (Fig. 2J and Suppl. Fig. 3C). However, transgenic BMSCs expressed three-fold more osteocalcin (*Bglap*) and two-fold more *Runx2* mRNA, respectively, compared to wild type BMSCs, suggesting a modest increase in osteoblastic differentiation potential (Suppl. Fig. 3D). The ratio of transgenic to endogenous *Prkg2* mRNA expression in BMSCs was similar to that found in bone (Suppl. Fig. 3E; compare to Fig. 1E).

Gender-specific differences in POB NO/cGMP generation and NO/cGMP serum concentrations

Previous workers showed that estradiol acutely increases endothelial NO production via membrane-bound estrogen receptor(ER)-α stimulation of NO synthase-3 (Russell *et al.* 2000; Mendelsohn & Karas 2010). Since POBs produce NO and cGMP constitutively (Rangaswami *et al.* 2009; Marathe *et al.* 2012; Joshua *et al.* 2014; Mendelsohn & Karas 2010), we hypothesized that female POBs, which contain higher ER-α copy numbers than males (Chaudhri *et al.* 2014), may produce more NO than male cells. Indeed, female POBs produced about 1.5-fold more nitrites and nitrates (stable NO metabolites) per hour per 10^6 cells compared to male POBs, and this correlated with increased phosphorylation of NOS-3 on Ser^{1179}, a stimulatory site (Fig. 3A,B). Correspondingly, the intracellular cGMP concentration was 1.7-fold higher in female compared to male POBs (Fig. 3C).

Estrogen replacement therapy in postmenopausal women increases NO_x and cGMP serum concentrations, and 24h urinary cGMP excretion (Hayashi *et al.* 2000; Rosselli *et al.* 1995; Mueck *et al.* 2001). Moreover, 24 h urinary cGMP excretion in pre-menopausal women is higher than in age-matched men (Cui *et al.* 2009; Markovitz *et al.* 1997). However, to our knowledge, gender-specific differences in serum NO_x and cGMP concentrations have not been examined. In eight week-old wild type and Col1a1-*Prkg2*^{RQ} transgenic mice, we found that NO_x and cGMP serum concentrations were 56% and 32% higher in female compared to male mice, respectively, with no significant difference between the two genotypes (Fig. 3D,E). Since PKG2 has a K_a for cGMP of about 0.4 μM (Fig. 1B) (Vaandrager *et al.* 2005), a change in cGMP concentration from 60 to 80 nM would be expected to increase PKG activity. These results suggest that females have higher endogenous PKG2 activities, at least in osteoblasts, but probably also in other tissues.

Increased trabecular bone mass in male Col1a1-*Prkg2*^{RQ} transgenic mice

Col1a1-*Prkg2*^{RQ} transgenic mice were born at the expected Mendelian frequency, were indistinguishable from their wild type littermates at birth, and showed no obvious skeletal abnormalities on plain X-Rays at eight weeks of age. They had similar body weights and tibial lengths as wild type mice, although the male transgenics showed a trend towards increased body weight (+ 4%, $p = 0.1$) (Fig. 4A,B). Computed tomography analysis of tibial bone micro-architecture revealed that eight week-old male transgenic mice had increased BMD (+20%), trabecular bone volume fraction (+47%), trabecular number (+27%), and trabecular thickness (+15%) compared to male wild type littermates (Fig. 4C,E). In contrast,

no apparent differences in trabecular micro-architecture were found between female transgenic and wild type mice at this age (Fig. 4D,F). Importantly, *Prkg2* mRNA and PKG2 protein expression were the same in bones and POBs from male and female Col1a1-*Prkg2*^{RQ} transgenic mice (data in Fig. 1F–H represent combined results from both sexes, but data were also analyzed separately). Cortical parameters (cortical bone area fraction, cross-sectional thickness and TMD) were the same in eight week-old transgenic and wild type mice of both genders (Suppl. Fig. 4A,B).

Increased bone formation parameters in male Col1a1-*Prkg2*^{RQ} transgenic mice

Consistent with the normal length of transgenic tibiae, femoral growth plate thickness was the same in male transgenic and wild type littermates (Fig. 5A,B). These results confirm lack of biologically-significant PKG2^{RQ} transgene expression in growth plate chondroblasts, and are in keeping with absence of Col1a1 promoter activity in the chondroblastic lineage (Kalajzic *et al.* 2002; Dacquin *et al.* 2002).

To determine the effect of PKG2^{RQ} expression on bone formation parameters, we performed histomorphometric measurements in the distal femur after double calcein labeling. Eight week-old male transgenic mice showed dramatically increased trabecular mineralizing surface (MS/BS, +91%), mineral apposition rate (MAR, +80%), and bone formation rate (BFR, +234%) compared to their male wild type littermates, suggesting both increased osteoblast numbers and activity (Fig. 5C). Similar results were found on endocortical bone surfaces (Suppl. Fig. 5A). The number of osteoblasts on trabecular as well as endocortical surfaces was increased by 71% and 97%, respectively, in male transgenic animals, while there was no change in osteoclast numbers (Fig. 5D,E).

Gender-specific increases in the expression of Wnt-related genes in male Col1a1-*Prkg2*^{RQ} transgenic mice

Pharmacologic activation of the NO/cGMP/PKG signaling cascade regulates the expression of Wnt-related genes in osteoblasts *in vitro* (Kalyanaraman *et al.* 2017; Rangaswami *et al.* 2012). In the tibiae of male wild type and Col1a1-*Prkg2*^{RQ} transgenic mice, mRNA expression of β-catenin (*Ctnnb1*), Wnt1, the Wnt co-receptor LRP5 (*Lrp5*), collagen-1α (*col1a1),* and alkaline phosphatase (*Alpl*) was increased two- to five-fold compared to male wild type tibiae; Wnt3a and osteocalcin (*Bglap*) mRNA showed a trend towards increased expression, while osteopontin (*Ssp1*) and β-actin (*Actb*) mRNA were unchanged (Fig. 5F). Expression of the β-catenin target gene cyclin D (*Ccnd1*) was increased >2-fold in transgenic bone, and *Fra-1* mRNA showed a trend towards increased expression (Fig. 5F), consistent with increased osteoblast proliferation. In contrast, in tibiae isolated from female mice, β-catenin mRNA was only 1.6-fold higher and the other mRNAs did not differ significantly between wild type and transgenic littermates (Suppl. Fig. 5B). Expression of the osteoclast regulators receptor of activated nuclear factor-Kb ligand (RANKL; gene name *Tnfsf11*) and osteoprotegerin (OPG; *Tnfrsf11b*), and of two osteoclast-specific genes—tartrate-resistant acid phosphatase (*Acp5*) and cathepsin K (*Ctsk*)—were the same in wild type and transgenic tibiae of both genders (Fig. 5G and Suppl. Fig. 5C).

Protection from diabetes-induced bone loss in male Col1a1-*Prkg2*^{RQ} transgenic mice

We recently demonstrated that the bone loss observed in male mice with type 1 diabetes is at least partly due to impaired NO/cGMP/PKG signaling in osteoblasts, and that restoring cGMP synthesis recovers depressed osteoblast functions in insulin-deficient animals (Kalyanaraman *et al.* 2018b). We focused on male mice to exclude the influence of estrogens on NO/cGMP signaling. To determine if increased PKG2 activity in osteoblasts is sufficient to protect Col1a1-*Prkg2*^{RQ} transgenic mice from diabetes-induced bone loss, we induced insulin deficiency by injecting 6 week-old male mice with streptozotocin (STZ). Mice were euthanized six weeks after STZ injections (Fig. 6A). Hyperglycemia was similar in STZ-treated transgenic mice and their wild type litter mates (Fig. 6B).

Wild type mice experienced diabetes-induced bone loss in both trabecular and cortical compartments (Fig. 6C,D), and this was associated with decreased bone formation parameters and decreased expression of osteoblast differentiation- and Wnt-related genes (Fig. 6E,F). Non-diabetic (vehicle-treated) male Col1a1-*Prkg2*^{RQ} transgenic mice showed higher trabecular and cortical bone volumes compared to their wild type litter mates (Fig. 6C,D). The increase in trabecular bone was similar in 8- and 12-week-old mice, but findings in cortical bone were more pronounced at 12 compared to 8 weeks of age (compare Fig. 6C,D to Fig. 4E and Suppl. Fig. 4A). In the transgenic mice, STZ-induced diabetes did not significantly affect trabecular bone and cortical bone area fraction; only cortical thickness and TMD decreased, but most values remained at least as high as those measured in control wild type mice (Fig. 6C,D). Similarly, bone formation parameters were elevated in transgenic control mice and remained high after induction of diabetes (Fig. 6E). The protection from bone loss and preservation of bone formation in diabetic Col1a1-*Prkg2*^{RQ} transgenic mice may relate, at least in part, to increased expression of osteoblast differentiation- and Wnt-related genes (including the β-catenin target gene cyclin D) (Fig. 6F).

DISCUSSION

Osteoblast-specific expression of a novel PKG2 mutant at a physiologically-relevant level

PKG2 deletions in humans and rodents cause dwarfism, and global PKG2 knockout mice exhibit a ~30% reduction in tibial and femoral length with profound growth plate abnormalities at 8 weeks of age; both genders appear equally affected (Pfeifer *et al.* 1996; Lipska *et al.* 2011; Bonnet *et al.* 2010). Eight week-old Col1a1-*Prkg2*^{RQ} transgenic mice had normal tibial length and growth plate architecture, consistent with specificity of the 2.3 kb fragment of the murine Col1a1 promoter for cells of the osteoblastic lineage (Dacquin *et al.* 2002; Kalajzic *et al.* 2002). In the mouse embryo, transcription from the 2.3kb Col1a1 promoter starts day 14 post conception in ossification centers, where osteoblasts differentiate and initiate bone mineralization (Dacquin *et al.* 2002). We cannot exclude adaptive developmental changes in the transgenic mice, but the absence of bone deformities and the relatively subtle changes in micro-architecture argue against major developmental changes.

The novel PKG2^{RQ} mutant had modestly increased kinase activity in the absence of cGMP and normal responsiveness to physiological increases in cGMP concentrations. We

confirmed tissue-specific expression of the transgene, producing about three-fold increased PKG2 protein and cGMP-stimulated kinase activity in transgenic *versus* wild type POB membranes. Phosphorylation of the PKG substrate VASP was increased in intact transgenic POBs to a degree similar to that seen when osteoblasts are mechanically stimulated or treated with estrogen (Rangaswami *et al.* 2010; Marathe *et al.* 2012). Thus, $PKG2^{RQ}$ activity was in a physiologically meaningful range, yet it had profound effects on osteoblast numbers and bone formation parameters. The PKG2 gain of function resulted in cell-autonomous increases in POB proliferation and resistance to apoptosis, explaining increased osteoblast numbers and bone formation rate *in vivo*.

Transgenic mice with chronically elevated plasma CNP concentrations exhibit a prominent skeletal overgrowth phenotype from excess PKG2 activity in growth plate chondroblasts (Kondo *et al.* 2015; Miyazawa *et al.* 2002). Since CNP also increases intracellular cGMP concentrations in primary osteoblasts, it is surprising that these mice do not have increased bone formation rates and show decreased trabecular bone volumes in the femurs of 8 week-old females (data on transgenic males were not reported) (Kondo *et al.* 2015). Whether CNP stimulates or inhibits osteoblast proliferation is controversial (Lenz *et al.* 2010; Hagiwara *et al.* 1996). The reason for these inconsistencies is unclear, but cGMP pools generated by soluble versus receptor GCs may be compartmentalized and differentially activate PKG1 and 2 in different cell types.

Gender-specific differences in the skeletal phenotype of Col1a1-*Prkg2*^{RQ} transgenic mice

Male mice expressing the *Prkg2*^{RQ} transgene had increased trabecular bone volumes and BMD at two and three months of age, whereas this phenotype was not evident in two month-old female mice. Despite similar $PKG2^{RQ}$ expression in male and female POBs and bones, we found gender-specific differences in nuclear β-catenin and Wnt/β-catenin-related gene expression. The sexual dimorphism of Col1a1-*Prkg2*^{RQ} transgenic mice likely relates to cross-talk between ER-α, NO/cGMP and Wnt/β-catenin signaling pathways (Kouzmenko *et al.* 2004; Mendelsohn & Karas 2010): First, estrogens increase NO (and cGMP) concentrations in endothelial cells and osteoblasts via ER-α activation of NO synthase (Marathe *et al.* 2012; Joshua *et al.* 2014; Mendelsohn & Karas 2010). Urinary cGMP excretion over 24 h is higher in pre-menopausal women compared to age-matched men (Cui *et al.* 2009; Markovitz *et al.* 1997), but, to our knowledge, there has been no prior direct comparison of serum or tissue NO/cGMP concentrations between males and females. We found higher serum NO and cGMP concentrations in female compared to male mice, consistent with our previous finding that ovariectomy decreases serum cGMP concentration while estrogen supplementation increases it (Joshua *et al.* 2014). Second, PKG2 directly and indirectly (via Akt) regulates GSK-3β activity, causing β-catenin stabilization, nuclear translocation, and induction of gene expression (Zhao *et al.* 2005; Kawasaki *et al.* 2008; Kalyanaraman *et al.* 2017). Female wild type POBs produced more NO and cGMP, and had more nuclear β-catenin compared to male POBs. The higher NO/cGMP activation of endogenous PKG2 may partly obscure the effects of PKG^{RQ} expression in female osteoblasts. Third, PKG2 activation by NO/cGMP increases mRNA and protein expression of the Wnt co-receptor LRP5 (Kalyanaraman *et al.* 2017). Increased *lrp5* expression likely contributed to the increased trabecular bone volume in male Col1a1-*Prkg2*^{RQ} transgenic

mice, because transgenic mice over-expressing wild type LRP5 show a similar increase in bone volume (Babij *et al.* 2003). Multiple reports indicate sexual dimorphism in Wnt/β-catenin signaling in bone, possibly caused by direct interactions between β-catenin and sex hormone receptors (Kouzmenko *et al.* 2004): (i) the low bone mass phenotype of LRP5 knockout mice and of transgenic mice over-expressing a Wnt inhibitor (secreted frizzled-related protein-1) is much more severe in males than females (Sawakami *et al.* 2006; Yao *et al.* 2010); (ii) the high bone mass phenotype of transgenic mice expressing wild type or constitutively-active LRP5 mutants shows gender-related differences (Babij *et al.* 2003; Dubrow *et al.* 2007); and (iii) human studies suggest that associations between genetic LRP5 variants and BMD are stronger in males than in females (Ferrari *et al.* 2004; Kiel *et al.* 2007). To fully understand the molecular basis of these gender-specific differences requires further investigation.

Protection from diabetic bone loss by osteoblast-specific PKG2^{RQ} expression

Low bone turn-over osteoporosis from impaired osteoblastic bone formation is a common complication of type 1 diabetes (Napoli *et al.* 2016). We have linked defective bone formation to decreased NO/cGMP/PKG signaling in osteoblasts under hyperglycemic conditions, and shown that *Prkg1 and 2* are both transcriptionally down-regulated in bones of insulin-deficient mice (Kalyanaraman *et al.* 2018b). Here, we provide evidence that increasing PKG2 activity in osteoblasts is sufficient to protect male mice from diabetic bone loss by restoring osteoblast proliferation and activity, in part by preventing down-regulation of Wnt/β-catenin signaling in diabetic bone. Thus, PKG2 appears to be the major cGMP target in diabetic bone.

Supplementary Material

Refer to Web version on PubMed Central for supplementary material.

Acknowledgments

We are grateful to Ella Kothari, Jennifer Santini, Dana Smith, and Dezhi Wang for their expert assistance.

Funding: This work was supported by NIH grants R01-AR051300 and R21-AR065658 (to RBP); P01-AG007996 (RLS), P30-CA023100 (UCSD Gene Targeting Mouse Core), P30-NS047101 (UCSD Neuroscience Microscopy Shared Facility), and P30-AR04603 (University of Alabama, Birmingham, Center for Metabolic Bone Disease). NS was supported by the Deutsche Forschungsgemeinschaft (Project KI 1303/2-1).

References

Aguirre J, Buttery L, O'Shaughnessy M, Afzal F, de Marticorena IF, Hukkanen M, Huang P, Maclntyre I, Polak J. Endothelial nitric oxide synthase gene-deficient mice demonstrate marked retardation in postnatal bone formation, reduced bone volume, and defects in osteoblast maturation and activity. Am J Pathol. 2001; 158:247–257. [PubMed: 11141498]

Armour KE, Armour KJ, Gallagher ME, Godecke A, Helfrich MH, Reid DM, Ralston SH. Defective bone formation and anabolic response to exogenous estrogen in mice with targeted disruption of endothelial nitric oxide synthase. Endocrinology. 2001; 142:760–766. [PubMed: 11159848]

Babij P, Zhao W, Small C, Kharode Y, Yaworsky PJ, Bouxsein ML, Reddy PS, Bodine PV, Robinson JA, Bhat B, Marzolf J, Moran RA, Bex F. High bone mass in mice expressing a mutant LRP5 gene. J Bone Miner Res. 2003; 18:960–974. [PubMed: 12817748]

Baron R, Kneissel M. WNT signaling in bone homeostasis and disease: from human mutations to treatments. Nat Med. 2013; 19:179–192. [PubMed: 23389618]

Bartels CF, Bukulmez H, Padayatti P, Rhee DK, van Ravenswaaij-Arts C, Pauli RM, Mundlos S, Chitayat D, Shih LY, Al-Gazali LI, et al. Mutations in the transmembrane natriuretic peptide receptor NPR-B impair skeletal growth and cause acromesomelic dysplasia, type Maroteaux. Am J Hum Genet. 2004; 75:27–34. [PubMed: 15146390]

Bocciardi R, Giorda R, Buttgereit J, Gimelli S, Divizia MT, Beri S, Garofalo S, Tavella S, Lerone M, Zuffardi O, et al. Overexpression of the C-type natriuretic peptide (CNP) is associated with overgrowth and bone anomalies in an individual with balanced t(2;7) translocation. Hum Mutat. 2007; 28:724–731. [PubMed: 17373680]

Bonnet C, Andrieux J, Beri-Dexheimer M, Leheup B, Boute O, Manouvrier S, Delobel B, Copin H, Receveur A, Mathieu M, Thiriez G, et al. Microdeletion at chromosome 4q21 defines a new emerging syndrome with marked growth restriction, mental retardation and absent or severely delayed speech. J Med Genet. 2010; 47:377–384. [PubMed: 20522426]

Bouxsein ML, Boyd SK, Christiansen BA, Guldberg RE, Jepsen KJ, Muller R. Guidelines for assessment of bone microstructure in rodents using micro-computed tomography. J Bone Miner Res. 2010; 25:1468–1486. [PubMed: 20533309]

Chaudhri RA, Schwartz N, Elbaradie K, Schwartz Z, Boyan BD. Role of ERa36 in membrane-associated signaling by estrogen. Steroids. 2014; 81:74–80. [PubMed: 24252378]

Chusho H, Tamura N, Ogawa Y, Yasoda A, Suda M, Miyazawa T, Nakamura K, Nakao K, Kurihara T, Komatsu Y, et al. Dwarfism and early death in mice lacking C-type natriuretic peptide. Proceedings of National Academy Science USA. 2001; 98:4016–4021.

Cui R, Iso H, Yamagishi K, Ohira T, Tanigawa T, Kitamura A, Kiyama M, Imano H, Konishi M, Shimamoto T. Relationship of urinary cGMP excretion with aging and menopausal status in a general population. J Atheroscler Thromb. 2009; 16:457–462. [PubMed: 19672035]

Dacquin R, Starbuck M, Schinke T, Karsenty G. Mouse a1(I)-collagen promoter is the best known promoter to drive efficient Cre recombinase expression in osteoblast. Dev Dyn. 2002; 224:245–251. [PubMed: 12112477]

Dubrow SA, Hruby PM, Akhter MP. Gender specific LRP5 influences on trabecular bone structure and strength. J Musculoskelet Neuronal Interact. 2007; 7:166–173. [PubMed: 17627087]

Ferrari SL, Deutsch S, Choudhury U, Chevalley T, Bonjour JP, Dermitzakis ET, Rizzoli R, Antonarakis SE. Polymorphisms in the low-density lipoprotein receptor-related protein 5 (LRP5) gene are associated with variation in vertebral bone mass, vertebral bone size, and stature in whites. Am J Hum Genet. 2004; 74:866–875. [PubMed: 15077203]

Grassi F, Fan X, Rahnert J, Weitzmann MN, Pacifici R, Nanes MS, Rubin J. Bone re/modeling is more dynamic in the endothelial nitric oxide synthase(-/-) mouse. Endocrinology. 2006; 147:4392–4399. [PubMed: 16763060]

Guo DC, Regalado E, Casteel DE, Santos-Cortez RL, Gong L, Kim JJ, Dyack S, Horne SG, Chang G, Jondeau G, et al. Recurrent gain-of-function mutation in PRKG1 causes thoracic aortic aneurysms and acute aortic dissections. Am J Hum Genet. 2013; 93:398–404. [PubMed: 23910461]

Hagiwara H, Inoue A, Yamaguchi A, Yokose S, Furuya M, Tanaka S, Hirose S. cGMP produced in response to ANP and CNP regulates proliferation and differentiation of osteoblastic cells. Am J Physiol. 1996; 270:C1311–C1318. [PubMed: 8967430]

Hannema SE, van Duyvenvoorde HA, Premsler T, Yang RB, Mueller TD, Gassner B, Oberwinkler H, Roelfsema F, Santen GW, Prickett T, et al. An activating mutation in the kinase homology domain of the natriuretic peptide receptor-2 causes extremely tall stature without skeletal deformities. J Clin Endocrinol Metab. 2013; 98:E1988–E1998. [PubMed: 24057292]

Hayashi T, Ito I, Kano H, Endo H, Iguchi A. Estriol (E3) replacement improves endothelial function and bone mineral density in very elderly women. J Gerontol A Biol Sci Med Sci. 2000; 55:B183–B190. [PubMed: 10811145]

Hofmann F, Bernhard D, Lukowski R, Weinmeister P. cGMP regulated protein kinases (cGK). Handb Exp Pharmacol. 2009:137–162.

Jamal SA, Cummings SR, Hawker GA. Isosorbide mononitrate increases bone formation and decreases bone resorption in postmenopausal women: a randomized trial. J Bone Miner Res. 2004; 19:1512–1517. [PubMed: 15312252]

Joshua J, Schwaerzer GK, Kalyanaraman H, Cory E, Sah RS, Li M, Vaida F, Boss GR, Pilz RB. Soluble guanylate cyclase as a novel treatment target for osteoporosis. Endocrinology. 2014; 155:4720–4730. [PubMed: 25188528]

Kalajzic I, Kalajzic Z, Kaliterna M, Gronowicz G, Clark SH, Lichtler AC, Rowe D. Use of type I collagen green fluorescent protein transgenes to identify subpopulations of cells at different stages of the osteoblast lineage. J Bone Miner Res. 2002; 17:15–25. [PubMed: 11771662]

Kalyanaraman H, Ramdani G, Joshua J, Schall N, Boss GR, Cory E, Sah RL, Casteel DE, Pilz RB. A Novel, Direct NO Donor Regulates Osteoblast and Osteoclast Functions and Increases Bone Mass in Ovariectomized Mice. J Bone Miner Res. 2017; 32:46–59. [PubMed: 27391172]

Kalyanaraman H, Schall N, Pilz RB. Nitric oxide and cyclic GMP functions in bone. Nitric Oxide. 2018a; 76:62–70. [PubMed: 29550520]

Kalyanaraman H, Schwaerzer G, Ramdani G, Castillo F, Scott BT, Dillmann W, Sah RL, Casteel DE, Pilz RB. Potein Kinase G Activation Reverses Oxidative Stress and Restores Osteoblast Function and Bone Formation in Male Mice With Type 1 Diabetes. Diabetes. 2018b; 67:607–623. [PubMed: 29301852]

Kalyanaraman H, Schwappacher R, Joshua J, Zhuang S, Scott BT, Klos M, Casteel DE, Frangos JA, Dillmann W, Boss GR, Pilz RB. Nongenomic thyroid hormone signaling occurs through a plasma membrane-localized receptor. Sci Signal. 2014; 7:ra48. [PubMed: 24847117]

Kawasaki Y, Kugimiya F, Chikuda H, Kamekura S, Ikeda T, Kawamura N, Saito T, Shinoda Y, Higashikawa A, Yano F, et al. Phosphorylation of GSK-3beta by cGMP-dependent protein kinase II promotes hypertrophic differentiation of murine chondrocytes. J Clin Invest. 2008; 118:2506–2515. [PubMed: 18551195]

Kiel DP, Ferrari SL, Cupples LA, Karasik D, Manen D, Imamovic A, Herbert AG, Dupuis J. Genetic variation at the low-density lipoprotein receptor-related protein 5 (LRP5) locus modulates Wnt signaling and the relationship of physical activity with bone mineral density in men. Bone. 2007; 40:587–596. [PubMed: 17137849]

Kondo E, Yasoda A, Fujii T, Nakao K, Yamashita Y, Ueda-Sakane Y, Kanamoto N, Miura M, Arai H, Mukoyama M, et al. Increased bone turnover and possible accelerated fracture healing in a murine model with an increased circulating C-type natriuretic peptide. Endocrinology. 2015; 156:2518–2529. [PubMed: 25860030]

Kouzmenko AP, Takeyama K, Ito S, Furutani T, Sawatsubashi S, Maki A, Suzuki E, Kawasaki Y, Akiyama T, Tabata T, Kato S. Wnt/beta-catenin and estrogen signaling converge in vivo. J Biol Chem. 2004; 279:40255–40258. [PubMed: 15304487]

Kuhn M. Molecular Physiology of Membrane Guanylyl Cyclase Receptors. Physiol Rev. 2016; 96:751–804. [PubMed: 27030537]

Lenz A, Bennett M, Skelton WP, Vesely DL. Vessel dilator and C-type natriuretic peptide enhance the proliferation of human osteoblasts. Pediatr Res. 2010; 68:405–408. [PubMed: 20613683]

Lipska BS, Brzeskwiniewicz M, Wierzba J, Morzuchi L, Piotrowski A, Limon J. 8.6Mb interstitial deletion of chromosome 4q13.3q21.23 in a boy with cognitive impairment, short stature, hearing loss, skeletal abnormalities and facial dysmorphism. Genet Couns. 2011; 22:353–363. [PubMed: 22303795]

Marathe N, Rangaswami H, Zhuang S, Boss GR, Pilz RB. Pro-survival Effects of 17beta-Estradiol on Osteocytes Are Mediated by Nitric Oxide/cGMP via Differential Actions of cGMP-dependent Protein Kinases I and II. J Biol Chem. 2012; 287:978–988. [PubMed: 22117068]

Markovitz JH, Lewis CE, Sanders PW, Tucker D, Warnock DG. Relationship of diastolic blood pressure with cyclic GMP excretion among young adults (the CARDIA Study): influence of a family history of hypertension. Coronary Artery Risk Development in Young Adults. J Hypertens. 1997; 15:955–962. [PubMed: 9321742]

Mendelsohn ME, Karas RH. Rapid progress for non-nuclear estrogen receptor signaling. J Clin Invest. 2010; 120:2277–2279. [PubMed: 20577045]

Miura K, Namba N, Fujiwara M, Ohata Y, Ishida H, Kitaoka T, Kubota T, Hirai H, Higuchi C, Tsumaki N, et al. An overgrowth disorder associated with excessive production of cGMP due to a gain-of-function mutation of the natriuretic peptide receptor 2 gene. PLoS ONE. 2012; 7:e42180. [PubMed: 22870295]

Miyazawa T, Ogawa Y, Chusho H, Yasoda A, Tamura N, Komatsu Y, Pfeifer A, Hofmann F, Nakao K. Cyclic GMP-dependent protein kinase II plays a critical role in C-type natriuretic peptide-mediated endochondral ossification. Endocrinology. 2002; 143:3604–3610. [PubMed: 12193576]

Mueck AO, Seeger H, Ludtke R, Graser T, Wallwiener D. Effect on biochemical vasoactive markers during postmenopausal hormone replacement therapy: estradiol versus estradiol/dienogest. Maturitas. 2001; 38:305–313. [PubMed: 11358648]

Nabhan AF, Rabie NH. Isosorbide mononitrate versus alendronate for postmenopausal osteoporosis. Int J Gynaecol Obstet. 2008; 103:213–216. [PubMed: 18805524]

Napoli N, Chandran M, Pierroz DD, Abrahamsen B, Schwartz AV, Ferrari SL. Mechanisms of diabetes mellitus-induced bone fragility. Nat Rev Endocrinol. 2016; 13:208–219. [PubMed: 27658727]

Pfeifer A, Aszòdi A, Seidler U, Ruth P, Hofmann F, Fässler R. Intestinal secretory defects and dwarfism in mice lacking cGMP-dependent protein kinase II. Science. 1996; 274:2082–2086. [PubMed: 8953039]

Rangaswami H, Marathe N, Zhuang S, Chen Y, Yeh JC, Frangos JA, Boss GR, Pilz RB. Type II cGMP-dependent protein kinase mediates osteoblast mechanotransduction. J Biol Chem. 2009; 284:14796–14808. [PubMed: 19282289]

Rangaswami H, Schwappacher R, Marathe N, Zhuang S, Casteel DE, Haas B, Chen Y, Pfeifer A, Kato H, Shattil S, et al. Cyclic GMP and protein kinase G control a Src-containing mechanosome in osteoblasts. Sci Signal. 2010; 3:ra91. [PubMed: 21177494]

Rangaswami H, Schwappacher R, Tran T, Chan GC, Zhuang S, Boss GR, Pilz RB. Protein Kinase G and Focal Adhesion Kinase Converge on Src/Akt/beta-Catenin Signaling Module in Osteoblast Mechanotransduction. J Biol Chem. 2012; 287:21509–21519. [PubMed: 22563076]

Rosselli M, Imthurn B, Keller PJ, Jackson EK, Dubey RK. Circulating nitric oxide (nitrite/nitrate) levels in postmenopausal women substituted with 17 beta-estradiol and norethisterone acetate. A two-year follow-up study. Hypertension. 1995; 25:848–853. [PubMed: 7721443]

Russell KS, Haynes MP, Sinha D, Clerisme E, Bender JR. Human vascular endothelial cells contain membrane binding sites for estradiol, which mediate rapid intracellular signaling. Proc Natl Acad Sci USA. 2000; 97:5930–5935. [PubMed: 10823945]

Sawakami K, Robling AG, Ai M, Pitner ND, Liu D, Warden SJ, Li J, Maye P, Rowe DW, Duncan RL, Warman ML, Turner CH. The Wnt co-receptor LRP5 is essential for skeletal mechanotransduction but not for the anabolic bone response to parathyroid hormone treatment. J Biol Chem. 2006; 281:23698–23711. [PubMed: 16790443]

Vaandrager AB, Ehlert EME, Jarchau T, Lohmann SM, De Jonge HR. N-terminal myristoylation is required for membrane localization of cGMP-dependent protein kinase type II. J Biol Chem. 1996; 271:7025–7029. [PubMed: 8636133]

Vaandrager AB, Hogema BM, De Jonge HR. Molecular properties and biological functions of cGMP-dependent protein kinase II. Front Biosci. 2005; 10:2150–2164. [PubMed: 15970484]

van't Hof RJ, Ralston SH. Nitric oxide and bone. Immunology. 2001; 103:255–261. [PubMed: 11454054]

Watanuki M, Sakai A, Sakata T, Tsurukami H, Miwa M, Uchida Y, Watanabe K, Ikeda K, Nakamura T. Role of inducible nitric oxide synthase in skeletal adaptation to acute increases in mechanical loading. J Bone Miner Res. 2002; 17:1015–1025. [PubMed: 12054156]

Wimalawansa SJ. Nitroglycerin therapy is as efficacious as standard estrogen replacement therapy (Premarin) in prevention of oophorectomy-induced bone loss: a human pilot clinical study. J Bone Miner Res. 2000; 15:2240–2244. [PubMed: 11092405]

Wimalawansa SJ. Rationale for using nitric oxide donor therapy for prevention of bone loss and treatment of osteoporosis in humans. Ann NY Acad Sci. 2007; 1117:283–297. [PubMed: 18056048]

Wimalawansa SJ, De MG, Gangula P, Yallampalli C. Nitric oxide donor alleviates ovariectomy-induced bone loss. Bone. 1996; 18:301–304. [PubMed: 8726385]

Yao W, Cheng Z, Shahnazari M, Dai W, Johnson ML, Lane NE. Overexpression of Secreted Frizzled-Related Protein 1 Inhibits Bone Formation and Attenuates PTH Bone Anabolic Effects. J Bone Miner Res. 2010; 25:190–199. [PubMed: 19594295]

Yuen SW, Chui AH, Wilson KJ, Yuan PM. Microanalysis of SDS-PAGE electroblotted proteins. BioTechniques. 1989; 7:74–83. [PubMed: 2629835]

Zhao X, Zhuang S, Chen Y, Boss GR, Pilz RB. Cyclic GMP-dependent protein kinase regulates CCAAT enhancer-binding protein beta functions through inhibition of glycogen synthase kinase-3. J Biol Chem. 2005; 280:32683–32692. [PubMed: 16055922]

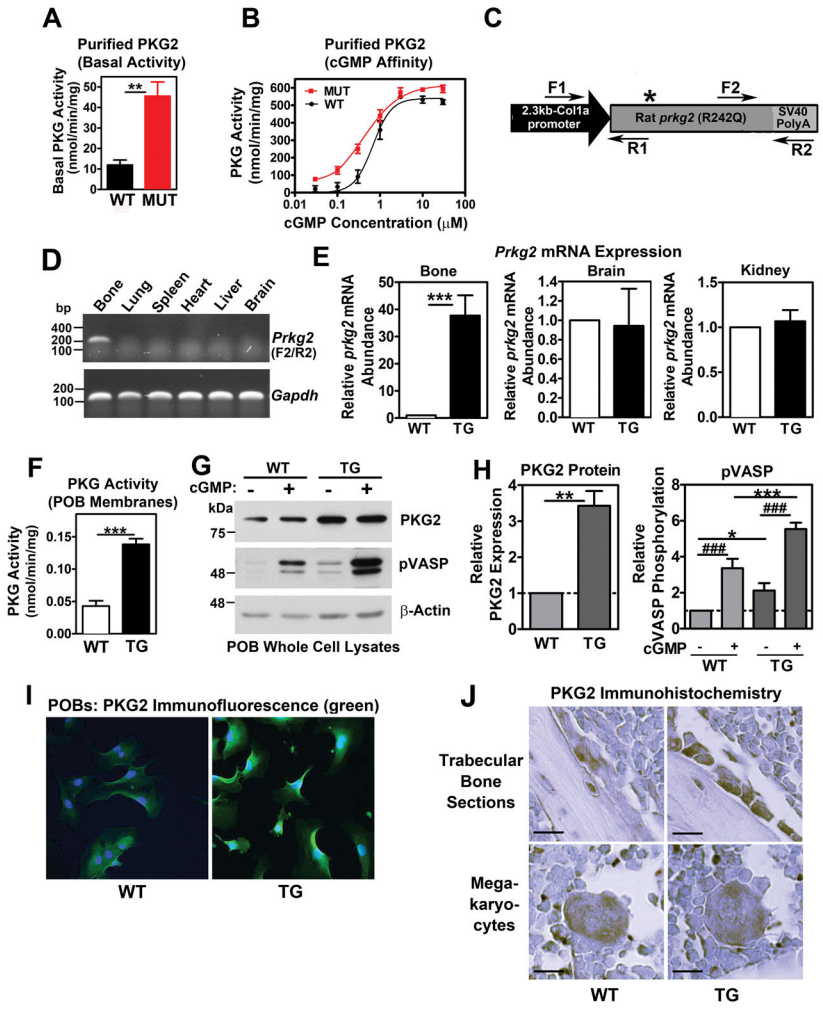

Fig. 1. Characterization of osteoblast-specific PKG2^{RQ} expression in transgenic Col1a1-*Prkg2*^{RQ} mice

(A,B) Wild type and mutant PKG2^{RQ} enzymes were affinity-purified from transfected 293T cells, and basal kinase activity was measured with a synthetic peptide in the absence of cGMP (A) or in the presence of increasing cGMP concentrations (B). **(C)** Scheme of the Col1a1-*Prkg2*^{RQ} construct used for injection into fertilized mouse eggs; the location of the R242Q mutation in the rat *Prkg2* cDNA is indicated by an asterisk. The positions of PCR primers used for genotyping (F1/R1) or detection of transgenic mRNA (F2/R2) are shown by arrows. **(D)** RNA was extracted from the indicated organs of a transgenic mouse, and transgene-derived mRNA was detected by RT-PCR using the F2/R2 primer pair shown in C. No PCR signal was obtained when reverse transcriptase was omitted (not shown); *Gapdh* served as a control for RNA quality. **(E)** RNA was extracted from bone, brain, and kidney of wild-type (WT) and transgenic (TG) mice, and *Prkg2* mRNA was quantified by qRT-PCR using primers recognizing both rat and mouse transcripts. Data were normalized to β2-microglobulin (*B2m*) and calculated according to the ΔΔCt method, assigning the mean of the WT group a value of one. Data are means ± SEM from n=10 mice per genotype for bone (5 males and 5 females) and n=4 for brain and kidney (***p<0.001). **(F)** Cell membranes were purified from primary osteoblasts (POBs) from WT and TG mice using a percoll

gradient, and cGMP-stimulated PKG activity was measured (mean ± SEM of three independent experiments; ***p<0.001). **(G,H)** POBs from WT and TG mice were serum-starved and treated with 100 μM 8-pCPT-cGMP (+cGMP) for 10 min. The amount of PKG2 protein and phosphorylation of the PKG substrate VASP on Ser^{239} were assessed by Western blotting of whole cell lysates, with β-actin serving as a loading control (G). Results of three independent POB isolates per genotype were quantified by densitometry scanning (H). Data represent means ± SEM (*p<0.05, **p<0.01, ***p<0.001, and $^{###}$p<0.001 for the indicated comparisons). **(I)** Immunofluorescence staining for PKG2 (green) in POBs isolated from WT and TG mice (nuclei counterstained with Hoechst 33342). **(J)** Immunohistochemical staining for PKG2 in tibial sections from WT and TG mice; top panels show osteoblasts on trabecular surfaces, bottom panels show megakaryocytes, which served as a positive control (bar = 20 μm). I and J are representative of POBs and bones from three mice per genotype.

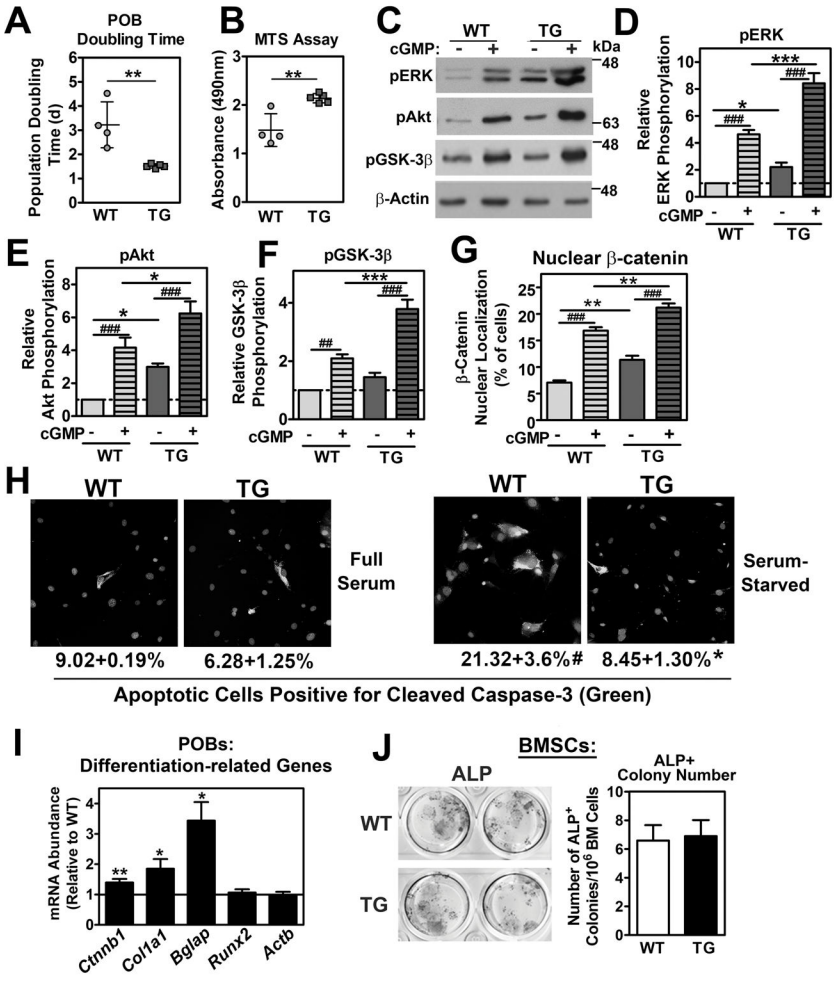

Fig. 2. Proliferation, Erk and Akt/GSK3/β-catenin signaling, survival, and differentiation of POBs isolated from male Col1a1-*Prkg2*^{RQ} transgenic and wild type POBs

POBs were isolated from eight week-old male transgenic (TG, n=5) and wild type (WT, n=4) mice. **(A,B)** Cells were plated at 1.2 × 10^5 cells/cm^2 and were counted 72 h later to calculate population doubling times (A). Metabolically-active cells were quantified by MTS reduction as described in Methods (B). Each data point represents the mean of three independent experiments performed with POBs from one mouse at passage 2 (lines show means ± SD; **p<0.01). **(C–F)** Serum-deprived POBs were treated with vehicle or 100 μM 8-pCPTcGMP (+cGMP) for 10 min. Western blots of cell extracts were analyzed with phospho-specific antibodies for ERK1/2-(pTyr^{204}), Akt(pSer^{473}), or GSK3β(pSer^9); β-actin served as a loading control. Bar graphs summarize results from three independent POB isolates per genotype. **(G)** Nuclear localization of β-catenin was determined by immunofluorescence staining of POBs isolated from three male mice per genotype. Bar graphs (D–G) show means ± SEM, *p/$^{\#}$p<0.05, **p/$^{\#\#}$p<0.01, and ***p/$^{\#\#\#}$p<0.001 for the indicated comparisons. **(H)** POBs were serum-starved for 24 h or kept in normal growth medium; apoptosis was detected by immunofluorescence staining for cleaved caspase-3 (green, nuclei counterstained with Hoechst 33342). The percentage of cells staining positive for cleaved caspase-3 is shown below (means ± SEM of three independent experiments;

$^{\#}p<0.05$ for comparison to wild type in full serum, and $*p<0.05$ for comparison to wild type serum-starved). **(I)** RNA was extracted from confluent POBs cultured in differentiation medium for 14 d; osteoblast differentiation-related transcripts were quantified by qRT-PCR and normalized to three housekeeping genes (18S, *hprt*, and *b2m*). Data were calculated according to the ΔΔCt method, with the mean of the WT group for each gene assigned a value of one. Gene names: *Ctnnb1* (β-catenin), *Col1a1* (collagen 1a1), *Bglap* (osteocalcin), and *Actb* (β-actin). **(J)** Bone marrow mononuclear cells from eight week-old male TG and WT mice (n = 5 mice of each genotype) were plated at 4×10^5 cells/cm^2, and adherent BMSCs were switched to osteoblastic differentiation medium. After 14 d, BMSC colonies were stained for ALP activity; the number of ALP+ colonies per well was counted and expressed per 10^6 bone marrow cells plated (means ± SEM; $*p<0.05$ and $**p<0.01$ for comparison to WT).

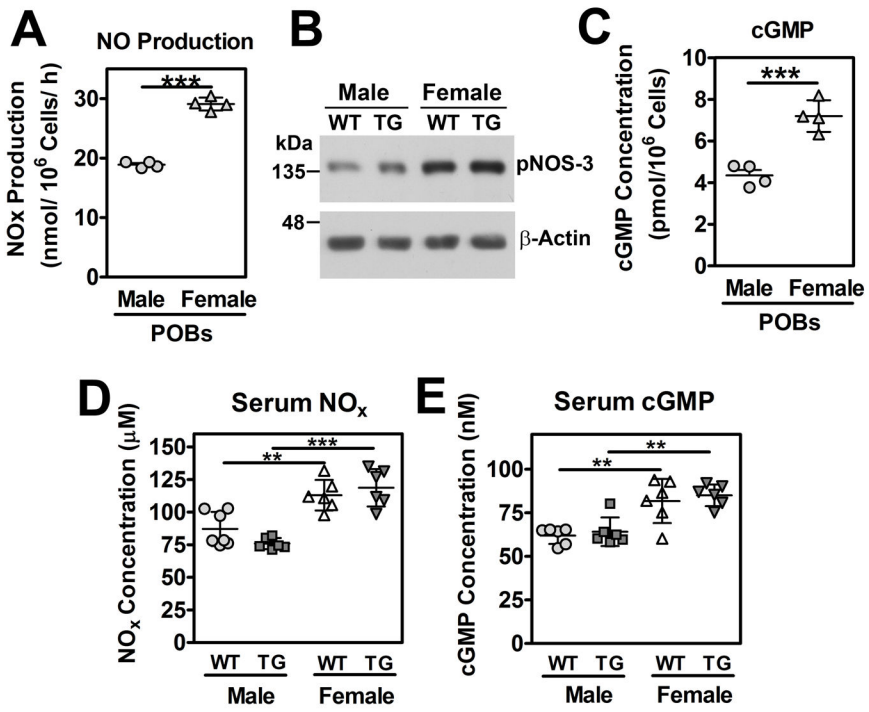

Fig. 3. Gender-specific differences in serum NOx and cGMP concentrations in mice

(A–C) POBs were isolated from 8 week-old male or female wild type mice (n=4 each) and were plated at passage 3 at equal density. Cells were transferred to fresh medium for 1 h prior to measuring NO_x (indicating the sum of nitrate plus nitrite) in the medium by Griess reaction (A). NOS-3 phosphorylation on Ser^{1799} was assessed in cell extracts by Western blotting with a phospho-specific antibody (B). Intracellular cGMP concentrations were measured by ELISA (C). **(D, E)** Serum was obtained by cardiac puncture at the time of euthanasia from male and female wild type (WT) and transgenic (TG) mice (n=6 per group). NO_x and cGMP concentrations were quantified by Griess reaction and ELISA, respectively. Data represent means ± SD (**p<0.01 and ***p<0.001 for the indicated comparisons).

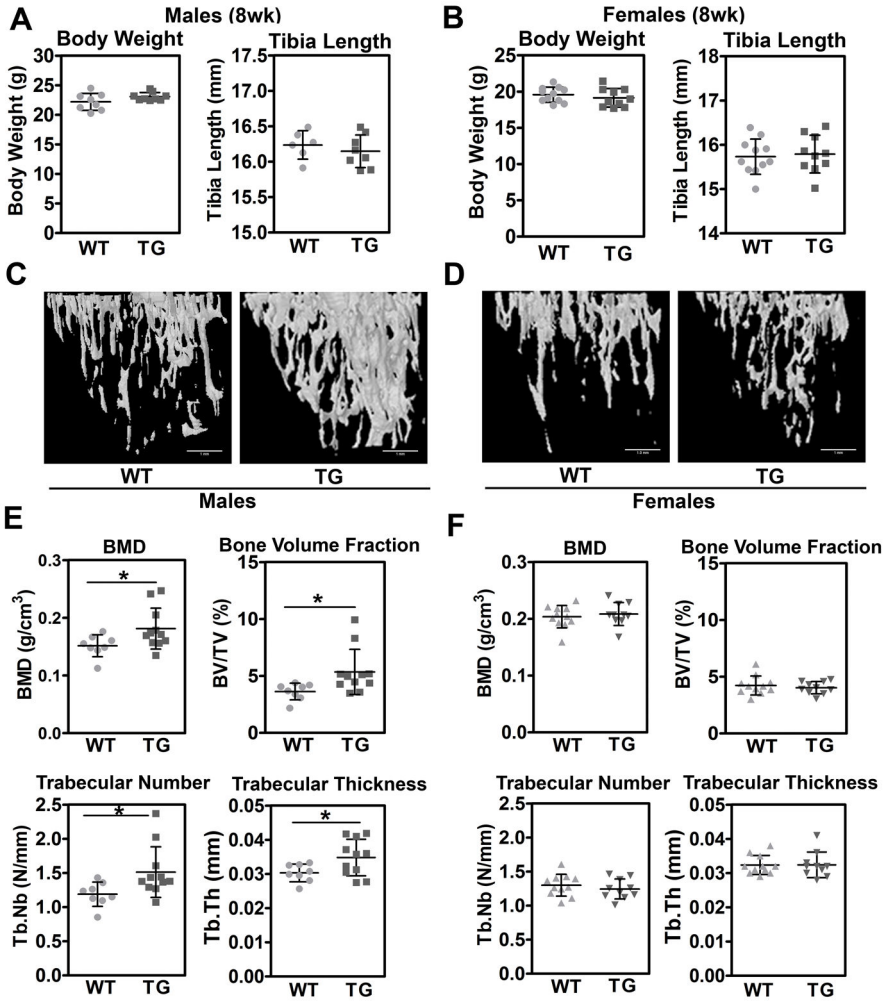

Fig. 4. Increased trabecular bone mass in male, but not female Col1a1-*Prkg2*^{RQ} transgenic mice

Male **(A,C,E)** and female **(B,D,F)** transgenic (TG) mice and their wild type (WT) litter mates were analyzed at eight weeks of age. **(A,B)** Body weight and tibia length are shown for each gender. **(C,D)** Tibiae were analyzed by micro-CT, with three-dimensional reconstruction of the trabecular bone at the proximal tibia below the growth plate shown. **(E,F)** Trabecular BMD, trabecular bone volume fraction (BV/TV), trabecular number (Tb.N), and trabecular thickness (Tb.Th) were measured by micro-CT at the proximal tibia. Data represent means ± SD (males: n=8 WT and n=10 TG; females: n=11 WT and n=10 TG). *p<0.05 for the indicated comparisons.

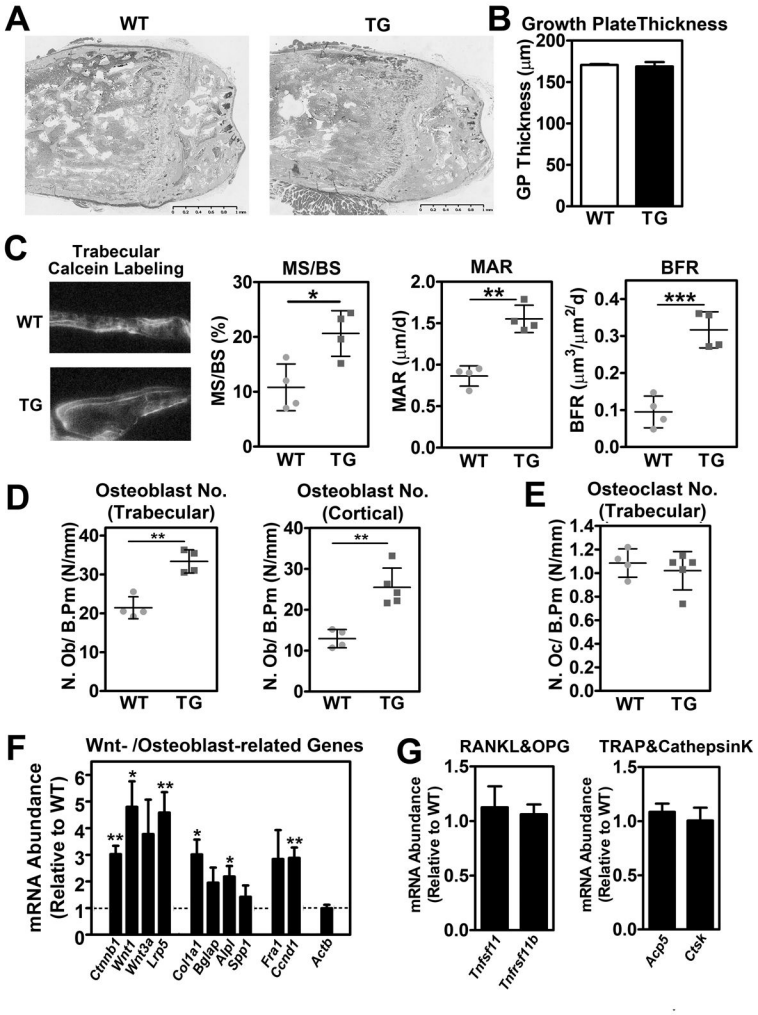

Fig. 5. Increased bone formation and expression of Wnt-related genes in male Col1a1-*Prkg2*^{RQ} transgenic mice

(A,B) Trichrome stains of distal femur sections were analyzed in 8 week-old male mice and the thickness of the growth plate was measured in the center and at three equally spaced points on each side (n=4 WT and n=5 TG). **(C)** Eight week-old males received calcein injections 7 and 2 d prior to euthanasia, and trabecular calcein labeling was assessed by fluorescence microscopy. Mineralizing surfaces (MS/BS), mineral apposition rates (MAR), and bone formation rates (BFR) were measured at trabecular surfaces between 0.25 and 1.25 mm proximal to the femoral growth plate. **(D,E)** Osteoblasts (D) were counted on femoral trabecular and endocortical surfaces, osteoclasts (E) on trabecular surfaces. Panels C-E show means ± SD of n=4 WT and n=5 TG mice; *p<0.05 and **p<0.01 by two sided t-test. **(F,G)** RNA was extracted from tibial shafts, and the relative abundance of Wnt-/osteoblast- and RANKL- or osteoclast-related transcripts was quantified by qRT-PCR and normalized to three different housekeeping genes (*18S*, *Hprt*, and *B2m*). Data were calculated according to the ΔΔCt method, with the mean of the WT group for each gene assigned a value of one. Gene names: *Ctnnb1* (β-catenin), *Bglap* (osteocalcin), *Alpl* (alkaline phosphatase), S*pp1* (osteopontin), *Ccnd1* (cyclin D1), *Actb* (β-actin), *Tnfsf11* (RANKL), T*nfrsf11b*

(osteoprotegerin), *Acp5* (tartrate-resistant acid phosphatase) and *Ctsk* (cathepsin K). Data represent means ± SEM from n=6 mice per genotype. *p<0.05 and **p<0.01 for the comparison between WT and TG mice (by two-sided t-test).

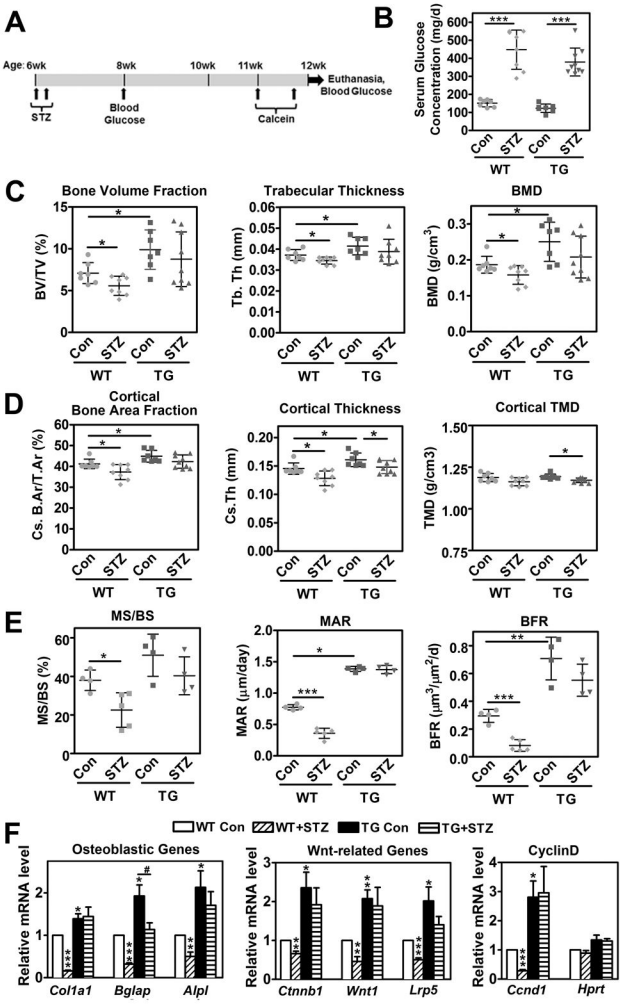

Fig. 6. Male Col1a1-*Prkg2*^{RQ} transgenic mice are protected from diabetes-induced bone loss

(A,B) Six-week-old male mice were injected with vehicle or streptozotocin (STZ, 100 mg/kg/d for two days) to induce type 1 diabetes. Blood glucose was measured 12 days later (B), and only hyperglycemic (>15 mM) STZ-treated mice were included in further analyses. All mice received calcein injections 7 and 2 d prior to euthanasia at the age of 12 weeks. **(C,D)** Tibiae were analyzed by micro-CT imaging (n=7 WT/control, n=8 WT/STZ, n=7 TG/control, n=9 TG/STZ). Trabecular bone volume fraction, trabecular thickness, and BMD were quantified by micro-CT at the proximal tibia (C). Cortical bone area fraction, cross-sectional thickness, and TMD were quantified at the mid-tibia (D). **(E)** Endocortical calcein labeling was assessed at the tibia, with quantification of mineralizing surfaces (MS/BS), mineral apposition rates (MAR), and bone formation rates (BFR) (n= 4–5 mice per group). Trabecular calcein labeling in diabetic mice was too weak to allow reliable quantification. Data in dot blots (B–E) represent means ± SD; *p<0.05, **p<0.01, ***p<0.001 for the indicated pair-wise comparisons. **(F)** RNA was extracted from tibial shafts. Relative mRNA abundance of osteoblastic and Wnt-related genes was quantified by qRT-PCR, as was expression of cyclin D (*Ccnd1*) and *Hpr*t. Gene expression was normalized to *18S* and data were calculated according to the ΔΔCt method, with the mean of the WT control group for

each gene assigned a value of one (n=6 mice per group; *p<0.05, **p<0.01, ***p<0.001 for the comparison to wild type control mice, #p<0.05 for the indicated comparison).